

Spin-induced strongly correlated magnetodielectricity, magnetostriction effect and spin-phonon coupling in helical magnet $\text{Fe}_3(\text{PO}_4)\text{O}_3$

Arkadeb Pal¹, C. H. Huang¹, T. W. Yen¹, P. H. Lee¹, Y. H. Chang¹, C. H. Yeh¹, T. W. Kuo¹, Ajay Tiwari¹, D. Chandrasekhar Kakarla¹, S. M. Huang¹, M. C. Chou², H. S. Kunwar³, S. Rana³, V. G. Sathe³, B. H. Chen⁴, Y. C. Chuang⁴, and H. D. Yang^{1,2#}

¹Department of Physics, National Sun Yat-sen University, Kaohsiung 804, Taiwan, R. O. C.

²Center of Crystal Research, National Sun Yat-sen University, Kaohsiung 804, Taiwan, R. O. C.

³UGC-DAE Consortium for Scientific Research, University Campus, Khandwa Road, Indore-452001, India

⁴National Synchrotron Radiation Research Center, Hsinchu, 30076, Taiwan, R. O. C.

#Corresponding author: yang@mail.nsysu.edu.tw

[**Key words:** Helical magnet, magnetodielectric coupling, T -dependent synchrotron XRD and Raman scattering, magnetostriction effect, spin-phonon coupling]

1. Introduction

The growing demand for futuristic spintronics devices with enhanced storage capacities and higher energy efficiencies has encouraged research on multifunctional materials that can respond to various external stimuli. Such materials display the coexistence of a broad spectrum of intriguing properties that often originate from cross-coupling of several microscopic order parameters such as spin, orbital, lattice, dipole, and phonon [1,2]. In this context, considerable research attention has been devoted to the discovery of new multiferroic and magnetodielectric materials, which largely help in envisaging many real-world applications [1,3–5]. To gain further insight into the relationship with magnetism, the magnetodielectric effect has been studied in various classes of magnetic systems [6]. In this regard, the compound $\text{Fe}_3\text{PO}_4\text{O}_3$ (FPO), known as mineral grattarolaite, may be of particular interest [7–9]. Previously, this compound was thought to be ordered in a commensurate collinear AFM phase [10]. Later, using neutron powder diffraction (NPD), Ross *et. al.* showed that FPO develops a highly anisotropic AFM helical spin structure (with domains having a needle-like correlation volume along the hexagonal c -axis) below $T_N \sim 163$ K [9]. Later, Sobolev *et. al.* further verified the helical magnetic ordering using Mössbauer spectroscopy [11]. Recently, a single-crystal neutron diffraction study of FPO suggested a special partial helical ordering with a wave vector having a well-defined magnitude but no preferred direction [12]; which is similar to the well-known B20 material MnSi [13]. In contrast to the extensively studied magnetic properties of FPO, a comprehensive study deciphering its dielectric, structural, and phononic properties are hitherto unreported. Nevertheless, owing to its spin-frustrated NCS structure and complex helical AFM magnetic ordering at an appreciably high temperature $T_N \sim 163$ K, FPO can be a unique playground to study a plethora of intriguing properties, including several of the strongly correlated phenomena such as magnetodielectric and/or magnetoelectric effect, SPC, and magnetostriction effect.

2. Technical Work

A solid state reaction method was used to prepare the sample FPO. In the reactions, dried high-purity (>99.99%, Alfa-Aesar) oxide powders of Fe_2O_3 , Ga_2O_3 , $\text{FeC}_2\text{O}_4 \cdot 2\text{H}_2\text{O}$, and $\text{NH}_4\text{H}_2\text{PO}_4$ were used as initial reagents in a stoichiometric ratio. The final products were initially checked for phase purity by collecting powder X-ray diffraction (XRD) data using a D8 Advance Bruker diffractometer ($\text{Cu-K}\alpha_1$, $\lambda = 1.54184 \text{ \AA}$). The XRD patterns at 300 K for both the aforementioned samples are shown in Fig. S1 in the supplemental material (SM). The temperature (T)-dependent synchrotron X-ray diffraction (SXRD) patterns were recorded at the Taiwan Photon Source (TPS) 19A beamline of the National Synchrotron Radiation Research Center (NSRRC), Taiwan, with an X-ray wavelength of 0.77489 \AA and a step-angle of 0.004° . To verify the phase and obtain several structural parameters, we performed a Rietveld analysis of both the XRD and SXRD data using the FullProf_suit program. The magnetization measurements were performed using a commercial SQUID-based magnetometer (MPMS, Quantum Design). Various dielectric measurements were carried out using a precision Agilent E4980A LCR meter with a helium-based closed-cycle-refrigerator (without a magnetic field) and a commercial Quantum Design MPMS with a homemade dielectric probe (under different magnetic fields). The pyrocurrent data were collected using a Keithley 6517A electrometer in a physical property measurement system (PPMS, quantum design). A Horiba Jobin Yvon HR-800 spectrometer equipped with an 1800 g/mm grating, an edge filter for Rayleigh line rejection, and a CCD detector was employed to record the Raman scattering data. A He-Ne laser (633 nm) beam focused onto a $\sim 2 \mu\text{m}$ diameter spot was used as the excitation source. The data were recorded in the backscattering geometry. The T -dependent

Raman measurements were carried out using a THMS600 stage from Linkam, U.K. with a temperature stability of ± 0.1 K.

Discussions:

Our study revealed that this system showed a pronounced dielectric anomaly at its magnetic transition temperature i.e., at 163 K, as shown in Fig. 1 (a) and Fig. 1(b). This is a clear magnetodielectric effect, which is originated due to the magnetostriction effect arising from the various exchange interactions below the magnetic ordering, i.e., 163 K, which is clear from Fig. 1 (c). Our Raman spectroscopy study also revealed a strong phonon renormalization occurring at its magnetic transition temperature in the form of anomalous phonon hardening and softening. Thus, our study unravels an interesting system showing strongly correlated behavior.

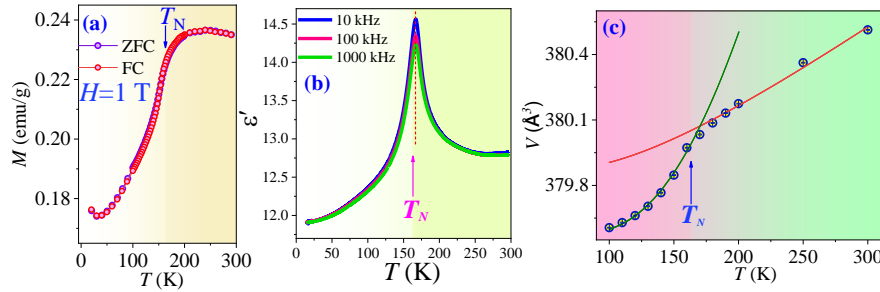


Figure. 1: (a) ZFC and FC $M(T)$ curves at $H=1$ T. (b) $\epsilon'(T)$ curves at various f under $H=0$ T. (c) displays the T -variations of the unit-cell volume V .

3. Conclusions

Here, we report a spectrum of simultaneously occurring and highly-entangled intriguing phenomena induced by helical spin ordering in a noncentrosymmetric and spin-frustrated system $\text{Fe}_3(\text{PO}_4)_3$. Such phenomena include magnetodielectric effect in the form of a frequency-independent pronounced dielectric peak, clear magnetostriction effect manifested as a dramatic down-turn in the thermal variation of lattice parameters, and strong spin-phonon coupling (which displays a unique anomalous hardening and softening of various phonon modes) at temperatures as high as $T_N=163$ K. The observed dielectric peak is seemingly associated to a structural distortion via the strong magnetostriction effect.

References

- [1] D. Khomskii, *Classifying Multiferroics: Mechanisms and Effects*, Physics (College. Park. Md). **2**, (2009).
- [2] B. Poojitha, A. Rathore, A. Kumar, and S. Saha, *Signatures of Magnetostriction and Spin-Phonon Coupling in Magnetolectric Hexagonal 15RBaMnO_3* , Phys. Rev. B **102**, 134436 (2020).
- [3] W. Eerenstein, N. D. Mathur, and J. F. Scott, *Multiferroic and Magnetolectric Materials*, Nature **442**, 759 (2006).
- [4] S.-W. Cheong and M. Mostovoy, *Multiferroics: A Magnetic Twist for Ferroelectricity*, Nat. Mater. **6**, 13 (2007).
- [5] H. C. Wu, K. D. Chandrasekhar, J. K. Yuan, J. R. Huang, J. Y. Lin, H. Berger, and H. D. Yang, *Anisotropic Spin-Flip-Induced Multiferroic Behavior in Kagome $\text{Cu}_3\text{Bi}(\text{SeO}_3)_2\text{O}_2\text{Cl}$* , Phys. Rev. B **95**, 2 (2017).
- [6] T. Aoyama, Y. Hasegawa, S. Kimura, T. Kimura, and K. Ohgushi, *Anisotropic Magnetodielectric Effect in the Honeycomb-Type Magnet -RuCl_3* , Phys. Rev. B **95**, 245104 (2017).
- [7] A. Modaresi, A. Courtois, R. Gerardin, B. Malaman, and C. Glezter, *Fe_3PO_7 , Un Cas de Coordinence 5 Du Fer Trivalent, Etude Structurale et Magnetique*, J. Solid State Chem. **47**, 245 (1983).
- [8] Q. Shi, L. Zhang, M. E. Schlesinger, J. Boerio-Goates, and B. F. Woodfield, *Low Temperature Heat Capacity Study of Fe_3PO_7 and $\text{Fe}_4(\text{P}_2\text{O}_7)_3$* , J. Chem. Thermodyn. **62**, 86 (2013).
- [9] K. A. Ross, M. M. Bordelon, G. Terho, and J. R. Neilson, *Nanosized Helical Magnetic Domains in Strongly Frustrated $\text{Fe}_3\text{PO}_4\text{O}_3$* , Phys. Rev. B **92**, 134419 (2015).
- [10] G. Gavoille, C. Glezter, and G. J. Long, *Revue de Chimie Min'erale* **24**, 42 (1987).
- [11] A. V. Sobolev, A. A. Akulenko, I. S. Glazkova, D. A. Pankratov, and I. A. Presniakov, *Modulated Magnetic Structure of Fe_3PO_7 as Seen by 57Fe Mössbauer Spectroscopy*, Phys. Rev. B **97**, 104415 (2018).
- [12] C. L. Sarkis, M. J. Tarne, J. R. Neilson, H. B. Cao, E. Coldren, M. P. Gelfand, and K. A. Ross, *Partial Antiferromagnetic Helical Order in Single-Crystal $\text{Fe}_3\text{PO}_4\text{O}_3$* , Phys. Rev. B **101**, 184417 (2020).
- [13] C. Pfleiderer, D. Reznik, L. Pintschovius, H.v. Löhneysen, M. Garst, and A. Rosch, *Partial Order in the Non-Fermi-Liquid Phase of MnSi* , Nature **427**, 227 (2004).